LETTERS
PUBLISHED ONLINE: 10 JANUARY 2010 | DOI: 10.1038/NGEO731
nature geoscience

The role of episodic overturn in generating the surface geology and heat flow on Enceladus

Craig O'Neill[1]* and Francis Nimmo[2]

The Saturnian satellite Enceladus is enigmatic in that its geologically active south polar region shows high heat flows[1] and geysers[2] not seen elsewhere on the satellite at present; its heavily deformed surface shows an episodic age distribution[2]; and the current observed heat loss exceeds the long-term tidal equilibrium heat production by a factor of at least 3.5 (ref. 3). These observations, which are not explained by existing convection models for Enceladus, suggest episodically active tectonism[4,5]. Here we present scaled numerical convection models of Enceladus's ice mantle, and show that all three observations are explained if convection is in a regime that involves occasional catastrophic overturns lasting about 10 million years, during which portions of the rigid ice lid are recycled into the interior, causing transiently enhanced heat loss. Our models show that episodic partial lid recycling occurs for plausible lid strengths and Enceladus's estimated supply of tidal energy. The localized nature of such overturn episodes, their periodicity of 0.1–1 billion years and an anomalous heat flow during these episodes are consistent with Enceladus's geology and heat supply. We propose that localized catastrophic overturn events may also explain the episodic partial resurfacing that has been inferred for other satellites, such as Ganymede, Rhea and Miranda.

The Cassini thermal imager measured a heat flow of 5.8 ± 1.9 GW emanating from the region south of 55° S (ref. 1; 9% of the surface area). The mean regional heat flux of 80 mW m^{-2} significantly exceeds the amount that can be transported by stagnant-lid convection[6]. The ultimate source of the heat is probably tidal dissipation within the ice shell[7–9], although tidally driven shear heating on near-surface faults may also contribute[10]. Irrespective of the heating mechanism, the global heat flow exceeds the 1.1 GW produced if Enceladus's eccentricity is in steady state[3] by almost an order of magnitude. Cratering statistics show a wide range of ages for Enceladus's surface. Heavily cratered plains yield ages of up to 4.2 billion years (Gyr), whereas the moderately cratered plains of Sarandib Planitia and Samarkand Sulcus yield ages of 170–3,750 million years (Myr) and 10–980 Myr, respectively[2]. The south pole terrain (SPT) is younger than 100 Myr, with estimates ranging down to 0.5 Myr, reflecting ongoing geological activity. Instead of being continuously active through time, the discrete ages of the different terrains imply that Enceladus experienced episodes of localized surface activity, interspersed with longer periods of relative inactivity[2]. On the basis of the cratering ages of these four terrains, activity seems to recur with a roughly ~1 Gyr periodicity. Palaeo heat-fluxes for older regions away from the south pole have been estimated at 200–270 mW m^{-2} (ref. 11) and 110–200 mW m^{-2} (ref. 12).

The high, localized heat fluxes and episodic surface age distribution are characteristics of Enceladus's tectonic evolution, and are not adequately explained by existing models. Classical stagnant-lid convection produces heat fluxes that are too small[13,14]. Classical mobile-lid convection[15] produces smooth age distributions, and also has the characteristic that the entire lid—or most of it—should be active, in contrast to observations on Enceladus. Thermochemical models so far do not reproduce the episodic age distribution observed[16]. Tidal heating can be localized by lateral variations in mechanical properties[8,9] or near-surface heating[17], but such models cannot reproduce the observed high heat fluxes or the episodic behaviour. All of the above models, and others (for example, ref. 10) also result in a balance between heat production and heat loss, which is violated by Enceladus[3]. The feedback between thermal and orbital evolution can result in periodic imbalances between heat production and heat loss, but the specific mechanism proposed in ref. 18 is insufficient to explain the anomaly[19] or the localization of tectonic activity. In contrast, episodic overturn can explain all of the observations.

Catastrophic, or episodic, overturn, is a transitional regime between mobile-lid and stagnant-lid convection[4]. The episodic regime arises if the yield stress of the lid, compared with the convective stresses, is too great to allow mobile-lid tectonics, but insufficient to ensure complete lid stagnation. This regime is characterized by occasional periods of high lid mobility in localized areas, and corresponding temporarily high heat fluxes[4].

To test the viability of this convection style for Enceladus, we used a two-dimensional Cartesian finite-element model to simulate convection in Enceladus's icy shell, as described in the Methods section. Figure 1 shows the basic model set-up and evolution of an Enceladus-like convecting system, with a basal Rayleigh number of around $\sim 8 \times 10^6$, based on the parameters shown in Table 1 and the figure caption. The physical model for Enceladus is based on refs 6, 13, 15 and 20. The key features of our model are temperature-dependent viscosity[21], and the Byerlee-style yielding behaviour of the near-surface ice layer. The convective stresses generated by this system are ~0.1 MPa, of a similar order to the lid strength. Establishment of a stable convective planform enables the convective thinning of portions of the lithosphere, and development of large variations in stagnant-lid thickness (Fig. 1a,b). The stagnant lid, being cold, is gravitationally unstable; and convection under the lid eventually results in a critical imbalance in lid thickness—thin and weak over upwellings, thick and gravitationally unstable over downwellings. This imbalance leads to brittle fracture and rupture of the lithosphere (Fig. 1c). A pulse of recycling ensues, lasting about 6 Myr and recycling ~45% of the surface (Fig. 1d), before the new lithosphere cools, homogeneously thickens and strengthens, and the system re-establishes itself under a stagnant lid (Fig. 1e). The behaviour is cyclic (Fig. 2), with pulses of lid regeneration recurring at intervals of between ~100 Myr and 2 Gyr, depending on the Rayleigh

[1]GEMOC, Department of Earth and Planetary Science, Macquarie University, Sydney, New South Wales 2109, Australia, [2]Department of Earth and Planetary Sciences, University of California Santa Cruz, Santa Cruz, California 95064, USA. *e-mail: coneill@els.mq.edu.au.

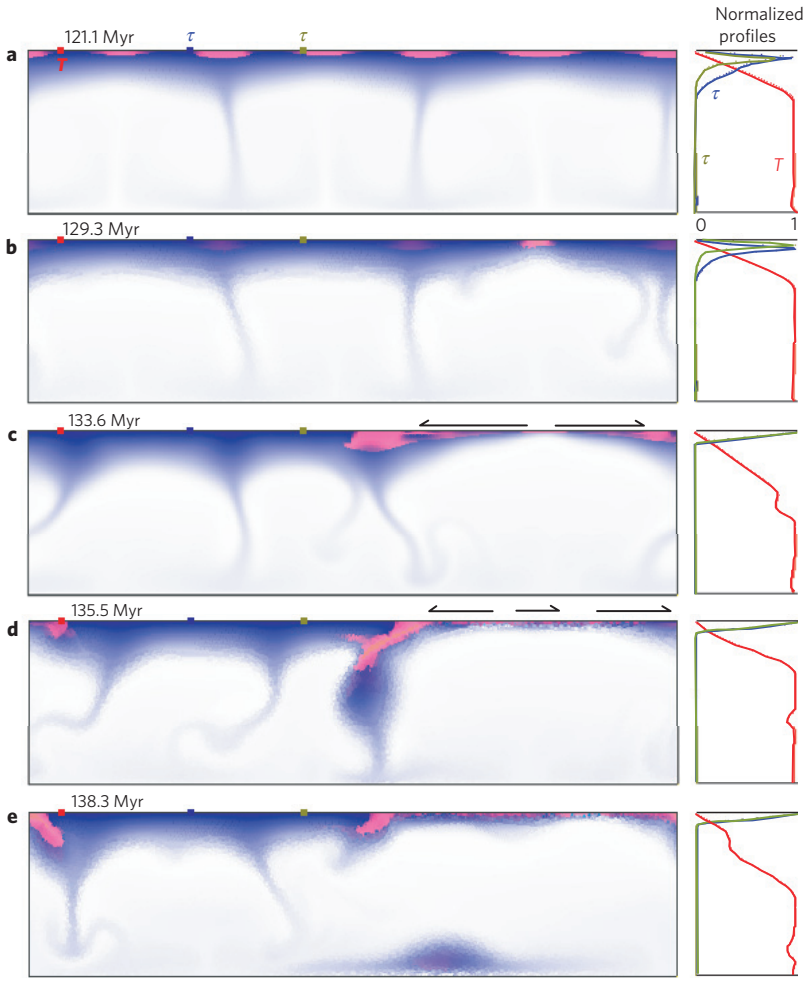

Figure 1 | Partial lid recycling during a catastrophic overturn event. a–e, Evolution of the temperature field (blue is cold; pink is plastically strained material) for a 4 × 1 aspect ratio simulation, demonstrating the partial lid recycling mechanism (depth is 92 km, width is 368 km). Model parameters from Table 1; the system Rayleigh number is $\sim 8.6 \times 10^6$; internal heat production rate is 1.15×10^{-10} W kg^{-1}; the effective friction coefficient $\mu = 0.1$. The normalized vertical profiles to the right of each image are for temperature (red) and stress (blue, green) against depth, at the sample points labelled in **a**. Surface velocities are indicated by black arrows in **c** and **d** (note that there are two spreading centres in **d**).

number, convective planform and yield stress properties. These short-duration (~10 Myr) periods of localized deformation and longer periods of quiescence are consistent with the Enceladus cratering statistics[2], and produce interior temperature fluctuations of around ~10–20 K. Figure 2a shows that during these recycling events, the global heat flux can equal or exceed that observed by Cassini[1]. Figure 2b demonstrates a significant spatial variation in heat flux, with the resurfacing region's heat flux comparable to that observed in Enceladus's SPT (ref. 1).

Figure 1 also demonstrates that partial lid recycling occurs, with critical thinning over only one upwelling, and associated lithospheric thickening on the edges of this active zone. In general, partial lid recycling of between 10 and 60% is observed in these models. The percentage of resurfaced lid depends strongly on the rheological stability of the non-spreading near-surface regions—if they are weak (that is, thinned), a large fraction of the lid can be recycled, whereas if they are reasonably strong and decoupled from the spreading regions by localized plastically failing zones, then the percentage of recycling during an overturn can be <40%.

The transition from inactive to episodically mobile-lid tectonics is a function of fault strength, and the internal vigour of the system (Fig. 3a). For strong faults ($\mu = 0.12$), or for sluggishly convecting systems ($\mu = 0.1, H < 0.5 \times 10^{-10}$ W kg^{-1}), surface deformation and resurfacing is not observed. For the equilibrium tidal heating rate[3]

Table 1 | Model parameters.

Surface temperature	T_s	70 K
Basal temperature*	T_b	270 K
Shell thickness	d	92 km
Basal viscosity	η	10^{14} Pa s
Viscosity contrast†	$\Delta\eta$	10^5 Pa s
Surface gravity	g	0.111 m s^{-2}
Ice density	ρ	950 kg m^{-3}
Thermal expansivity	α	5×10^{-5} K^{-1}
Diffusivity	κ	1×10^{-6} m^2 s^{-1}
Heat capacity	C_p	1,500 J kg^{-1} K^{-1}
Heat production‡	H	10^{-11} (min.) – 2.3×10^{-10} (max.) W kg^{-1}
Fault friction coefficient§	μ	0.08 (min.) – 0.16 (max.)

*Assumes the presence of liquid water at the base of the ice shell (although an ocean is not required for this model to work).

†Frank–Kamenetski approximation, approximates a high-contrast Arrhenius dependence over a rheologically active layer.

‡Assumed constant here, but the range encompasses integrated values over resonance and non-resonance periods.

§Coefficient for a pressure-dependent Byerlee-style yield criterion.

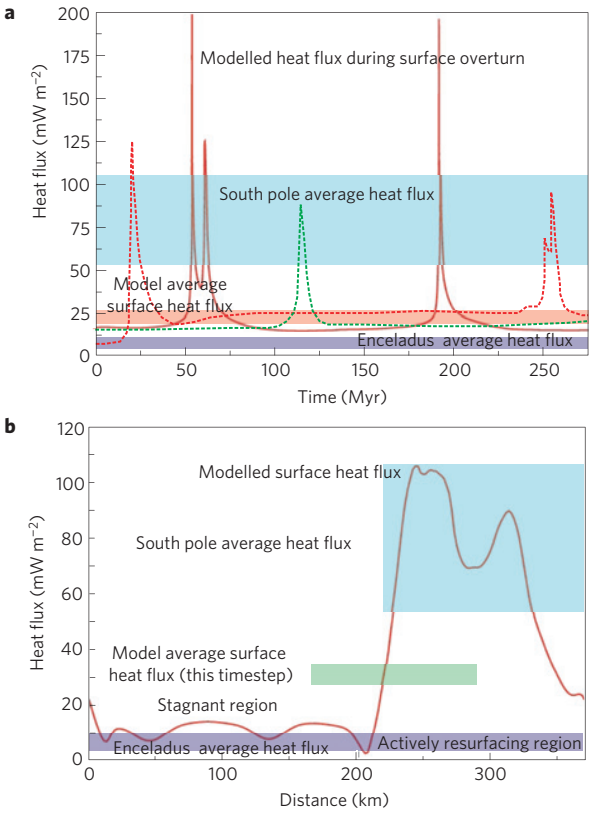

Figure 2 | Behaviour of heat flux during a catastrophic overturn event. **a**, Modelled heat flux versus time for episodic systems with different aspect ratios of 1×1 (red line), 4×1 (green dashed line) and 8×1 (red dashed line). As per Fig. 1, with internal heat production of 2.3×10^{-10} W kg^{-1}. Large-scale lid recycling enables the upwelling of warm material to the near surface, resulting in a pulse of surface heat flux far beyond the normal background rate. Also shown are the 1×1 model's average surface heat flux over the simulation (red rectangle), Enceladus's estimated globally averaged heat flux (7 mW m^{-2}, purple rectangle) and the present heat flux of the SPT (54–106 mW m^{-2}, cyan rectangle). **b**, Transect of heat flux along the surface of the model in Fig. 1d, illustrating the regionally elevated heat flux of an actively overturning surface. The average heat flux for this timestep is in green, otherwise as in **a**.

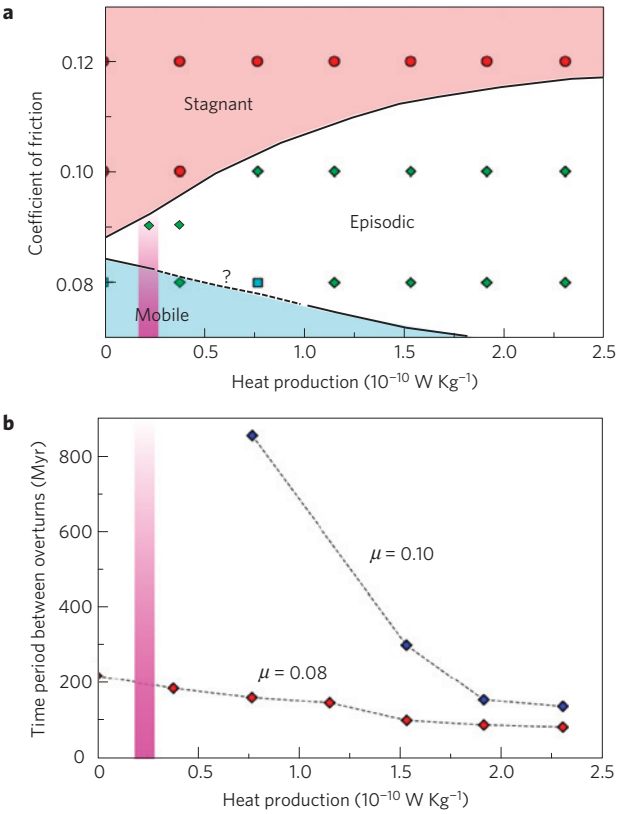

Figure 3 | Tectonic regime and periodicity of overturns as a function of model parameters. **a**, Tectonic regime of Enceladus-like convecting systems (symbols labelled) as a function of heat production and friction coefficient μ. Models were run at 1×1 aspect ratios; parameters from Table 1. Enceladus's equilibrium tidal heat production[3] is 2.3×10^{-11} W kg^{-1} (pink rectangle). **b**, The effect of heat production rate on the interval between overturns. The points plotted on the $\mu = 0.08$ trend corresponding to heat production values of 0 and 0.767×10^{-10} W kg^{-1} eventually settled into a mobile-lid regime after initial overturns. The cratering record indicates at least four distinct resurfacing episodes on Enceladus, with an interval of ~1 Gyr (see text). For the long-term tidal heat production rate of 0.23×10^{-10} W kg^{-1} (ref. 3), a recurrence interval of ~1 Gyr implies $\mu \approx 0.09$.

of 0.23×10^{-10} W kg^{-1}, $\mu \approx 0.09$ will permit an episodic overturn regime. The recurrence interval of catastrophic overturns is sensitive to energy dissipation in the system, particularly the work done by faulting, and internal energy production (Fig. 3b). Although not tightly constrained, Enceladus seems to have had at least four distinct resurfacing episodes[2], which gives a recurrence interval of ~1 Gyr. For an appropriate fault strength ($\mu = 0.09$), Fig. 3b suggests that the equilibrium tidal heating rate is roughly consistent with a ~1 Gyr recurrence interval, although this depends on the basal Rayleigh number, fault strength and internal heat production. The values for μ that we require are smaller than the standard static value of ~0.6 (ref. 22). However, for faults of a few kilometres depth[10] our values for μ give a yield strength of ~0.01–0.1 MPa, comparable to the stresses required to cause cycloidal ridge propagation on Europa[23] and shear failure on Enceladus[24].

Episodic convection of the kind proposed here can explain the localized nature of the south polar thermal anomaly, the present-day high heat flux and the apparently episodic nature of deformation on Enceladus. In particular, the long-term equilibrium tidal heating rate[3] permits episodic, high heat flux episodes as long as the ice shell is relatively weak ($\mu \approx 0.09$). The south polar location of the current anomaly is probably due to enhanced tidal heating there[6,8], and this location may change with the redistribution of mass within Enceladus's interior[20]. Note that the tidal heating in our models is simply prescribed uniformly for the whole system. To fully understand the south-pole localization will require a three-dimensional spherical model for Enceladus; the overturn periodicity varies not only with yield stress (Fig. 3), or, more subtly, with the geometrical configuration (Fig. 2), but also varies within any given model run owing to nonlinearities in the convecting system, although the basic episodic mechanism is not unduly sensitive to geometry[25].

Geological observations of the SPT provide some support for the model. The margins of the SPT have been interpreted as convergent features[2,26], consistent with our model, and the localization of geological activity to the SPT is consistent with thinning of the lithosphere over a convective upwelling (for example, ref. 20).

Episodic resurfacing persists for only ~10 Myr (Fig. 2), which is consistent with the young surface age of the SPT, but suggests that we are viewing Enceladus during the ~1–10% of the time it undergoes resurfacing. Such episodic activity is also suggested by the rapid current inferred rate of ^{40}Ar loss[27] and the apparently short (~10 Myr) lifetime of the putative subsurface ocean[28]. The current geyser-driven mass escape rate is apparently insufficient

to resupply the E ring[2], suggesting that resurfacing activity is now in its waning phase. E ring particles are apparently responsible for the high albedo of Tethys and Enceladus[29]; if the geysers have operated only intermittently, then this brightness may also be a recent phenomenon. Finally, several other icy satellites in the outer solar system, notably Ganymede, Rhea and Miranda, show tectonic deformation and variations in surface ages suggestive of partial resurfacing[30]. Episodic overturn may thus have had a key role in sculpting these bodies' surfaces.

Methods

We use a Lagrangian integration point finite-element code (Ellipsis, for example, ref. 4) to carry out our convection calculations. The grid resolution is 64×254, with a grid refinement factor of 0.6 in the near-surface zone. Courant timestepping is used, with a maximum viscosity contrast of five orders of magnitude, but <10 over any cell. Free slip isothermal top and bottom boundary conditions, and periodic (wrap-around) side boundary conditions are used. An example is shown in Fig. 1. In this model the temperature field is shown; blue indicates cold material (dimensionless temperature < 0.5) and pink tones indicate material under plastic strain (stress > yield stress at given pressure).

For high coefficients of friction, the lid's strength prevents its mobilization and convection is in a stagnant lid. For extremely weak lids with low coefficients of friction, and low heat production, convection entered into the mobile-lid regime. For intermediate fault strengths ($\mu \sim 0.1$) and the range of heat production rates modelled, convection is in an episodic regime characterized by sporadic, catastrophic overturns during which the lid (or large portions of it) is recycled. Tidal heating is implemented by assuming a constant internal heat production rate for the icy shell, with values spanning the range from primarily bottom heating (10^{-11} W kg^{-1}), to significant tidal heating concentrated in the ice shell (2.3×10^{-10} W kg^{-1}). This range gives us appropriate background heat fluxes for Enceladus ($\sim$7 mW m^{-2} based on the global heat budget[1], up to 20 mW m^{-2} based on stagnant-lid models[13]). For more widely spaced episodic events, the modelled average heat flux approaches Enceladus's average.

Received 15 June 2009; accepted 24 November 2009; published online 10 January 2010

References

1. Spencer, J. R. *et al.* Cassini encounters Enceladus: Background and the discovery of a south polar hot spot. *Science* **311,** 1401–1405 (2006).
2. Porco, C. C. *et al.* Cassini observes the active south pole of Enceladus. *Science* **311,** 1393–1401 (2006).
3. Meyer, J. & Wisdom, J. Tidal heating in Enceladus. *Icarus* **188,** 535–539 (2007).
4. Moresi, L. & Solomatov, V. S. Mantle convection with a brittle lithosphere: Thoughts on the global tectonic styles of the Earth and Venus. *Geophys. J. Int.* **133,** 669–682 (1998).
5. Trompert, R. & Hansen, U. Mantle convection simulations with rheologies that generate plate-like behaviour. *Nature* **395,** 686–689 (1998).
6. Roberts, J. & Nimmo, F. Tidal heating and the long-term stability of a subsurface ocean on Enceladus. *Icarus* **194,** 675–689 (2008).
7. Ross, M. & Schubert, G. Viscoelastic models of tidal heating in Enceladus. *Icarus* **78,** 90–101 (1989).
8. Tobie, G. *et al.* Solid tidal friction above a liquid water reservoir as the origin of the south pole hotspot on Enceladus. *Icarus* **196,** 642–652 (2008).
9. Mitri, G. & Showman, A. P. A model for the temperature-dependence of tidal dissipation in convective plumes on icy satellites: Implications for Europa and Enceladus. *Icarus* **195,** 758–764 (2008).
10. Nimmo, F. *et al.* Shear heating as the origin of the plumes and heat flux on Enceladus. *Nature* **447,** 289–291 (2007).
11. Giese, B. *et al.* Enceladus: An estimate of heat flux and lithospheric thickness from flexurally supported topography. *Geophys. Res. Lett.* **53,** L24204 (2008).
12. Bland, M. *et al.* Unstable extension of Enceladus' lithosphere. *Icarus* **192,** 92–105 (2007).
13. Barr, A. C. & McKinnon, W. B. Convection in Enceladus' ice shell: Conditions for initiation. *Geophys. Res. Lett.* **34,** L09202 (2007).
14. Grott, M. *et al.* Degree-one convection and the origin of Enceladus' dichotomy. *Icarus* **191,** 203–210 (2007).
15. Barr, A. C. Mobile lid convection beneath Enceladus' south polar terrain. *J. Geophy. Res.* **113,** E07009 (2008).
16. Stegman, D. R., Freeman, J. & May, D. A. Origin of ice diapirism, true polar wander, subsurface ocean and tiger stripes of Enceladus driven by compositional convection. *Icarus* **202,** 669–680 (2009).
17. Roberts, J. H. & Nimmo, F. Near-surface heating on Enceladus and the south polar thermal anomaly. *Geophys. Res. Lett.* **35,** L09201 (2008).
18. Ojakangas, G. W. & Stevenson, D. J. Thermal state of an ice shell on Europa. *Icarus* **81,** 220–241 (1989).
19. Meyer, J. & Wisdom, J. Episodic volcanism on Enceladus: Application of the Ojakangas-Stevenson model. *Icarus* **198,** 178–180 (2008).
20. Nimmo, F. & Pappalardo, R. T. Diapir-induced reorientation of Saturn's moon Enceladus. *Nature* **441,** 614–616 (2006).
21. Moresi, L. *et al.* A Lagrangian integration point finite element method for large deformation modeling of viscoelastic geomaterials. *J. Comput. Phys.* **184,** 476–497 (2003).
22. Beeman, M. *et al.* Friction of ice. *J. Geophys. Res.* **93,** 7625–7633 (1988).
23. Hoppa, G. V. *et al.* Formation of cycloidal features on Europa. *Science* **285,** 1899–1902 (1999).
24. Smith-Konter, B. & Pappalardo, R. T. Tidally driven stress accumulation and shear failure of Enceladus's tiger stripes. *Icarus* **198,** 435–451 (2008).
25. Stein, C. *et al.* The effect of rheological parameters on plate behaviour in a self-consistent model of mantle convection. *Phys. Earth Planet. Int.* **142,** 225–255 (2004).
26. Helfenstein, P. *et al.* Patterns of fracture and tectonic convergence near the South Pole of Enceladus. *Lunar Planet. Sci. Conf.* **37,** abstr. 2182 (2006).
27. Waite, J. H. *et al.* Liquid water on Enceladus from observations of ammonia and Ar-40 in the plume. *Nature* **460,** 487–490 (2009).
28. Roberts, J. H. & Nimmo, F. Tidal heating and the long-term stability of subsurface ocean on Enceladus. *Icarus* **194,** 675–689 (2008).
29. Verbiscer, A. J. *et al.* The opposition surge of Enceladus: HST observations 338–1022 nm. *Icarus* **173,** 66–83 (2005).
30. Collins, G. C. *et al.* in *Planetary Tectonics* (eds Schultz, R. A. & Watters, T. R.) (Cambridge Univ. Press, in the press).

Acknowledgements

C.O. acknowledges ARC support, GEMOC publication no. 621. F.N. acknowledges NASA Outer Planets Research support.

Author contributions

C.O. and F.N. contributed to the paper writing. C.O. carried out the numerical calculations.

Additional information

The authors declare no competing financial interests. Reprints and permissions information is available online at http://npg.nature.com/reprintsandpermissions. Correspondence and requests for materials should be addressed to C.O.